

UC San Diego

UC San Diego Electronic Theses and Dissertations

Title

Design of a Portable Shape Display for Augmented Reality

Permalink

<https://escholarship.org/uc/item/9xt2w6fv>

Author

Tsui, Tse

Publication Date

2020

Supplemental Material

<https://escholarship.org/uc/item/9xt2w6fv#supplemental>

Peer reviewed|Thesis/dissertation

UNIVERSITY OF CALIFORNIA SAN DIEGO

Design of a Portable Shape Display for Augmented Reality

A thesis submitted in partial satisfaction of the
requirements for the degree of Master of Science

in

Engineering Sciences (Mechanical Engineering)

by

Tse Tsui

Committee in charge:

Professor Tania Morimoto, Chair
Professor Nicholas Gravish
Professor Michael Tolley

2020

Copyright

Tse Tsui, 2020

All rights reserved.

The Thesis of Tse Tsui is approved, and it is acceptable in quality and form for publication on microfilm and electronically:

Chair

University of California San Diego

2020

DEDICATION

This thesis is wholeheartedly dedicated to my beloved parents, who continuously provide their moral, spiritual, emotional, and financial support.

To my younger sister, girlfriend, relatives, and friends who shared their accompany and encouragement to finish my study.

TABLE OF CONTENTS

Signature Page	iii
Dedication	iv
Table of Contents	v
List of Figures	vii
List of Tables	viii
Acknowledgements	ix
Abstract of the Thesis	x
Chapter 1 Introduction	1
1.1 Grounded Haptic Devices	3
1.2 Ungrounded Haptic Devices	4
1.3 Encountered Type Haptic Display	6
1.4 Contributions	6
Chapter 2 System Design	7
2.1 Hardware Design	7
2.2 Software and Electronics	10
2.3 Shape Rendering Method	11
Chapter 3 Device Parameter User Study	14
3.1 Device Setup	15
3.2 Experimental Procedure	16
3.3 Pin Size Experiment	17
3.3.1 Experimental Setup	17
3.3.2 Results and Discussion	17
3.4 Pin Shape Experiment	19
3.4.1 Experimental Setup	19
3.4.2 Results and Discussion	19
3.5 Contact Foam Stiffness Experiment	20
3.5.1 Experimental Setup	20
3.5.2 Results and Discussion	20
Chapter 4 Object Identification User Study	21
4.1 Experimental Procedure	21
4.2 Results	22
Chapter 5 Preliminary Application	24

5.1	Dynamic Surface Demonstration	24
5.2	Mass Spring Damper Demonstration	25
Chapter 6	Conclusions and Future Work	27
Bibliography	29

LIST OF FIGURES

Figure 1.1.	Device overview.....	2
Figure 2.1.	Hardware Overview.....	8
Figure 2.2.	Hardware Detail.....	9
Figure 2.3.	Pin and phone mount.....	10
Figure 2.4.	System Diagram.....	11
Figure 2.5.	Rendering Method.....	12
Figure 3.1.	Non-mechatronic version of the device for device parameters user study .	15
Figure 3.2.	Time lapse of using non-mechatronic version of the device	16
Figure 3.3.	Data of device parameters user study in horizontal bar chart	18
Figure 4.1.	Object identification user study results	22
Figure 5.1.	Dynamice surface	25
Figure 5.2.	MSD system.....	26

LIST OF TABLES

Table 3.1.	Parameters used in device parameters user study	17
Table 3.2.	Device parameters user study results	19
Table 4.1.	Object identification user study analysis	23

ACKNOWLEDGEMENTS

First, I would like to express my deep and sincere gratitude to Professor Morimoto for her continuous support and guidance in overcoming numerous obstacles throughout my M.S study and research. Her haptic interface course led me into my research direction and provided the inspiration for this thesis. She has not only provided me with the mentor-ship that has helped me to develop this work to its full potential, but also been a consistent role model for me as I develop professionally and learn what it means to be an academic researcher. I am also grateful to have a reader position in her linear control course which both helped to support my education as well as solidify my understanding of the subject. I could not have imagined having a better advisor and mentor for my M.S study.

Additionally, I would like to thank the other members of my committee. In particular, I would like to thank Professor Tolley, whose introduction to robotics course helped me build a solid foundation of knowledge in the robotics area. I would also like to thank Professor Gravlish, whose bioinspired mobile robotics course has inspired me to consider new research possibilities for the future.

Further, I would also like to thank all the members of the Moromoto Lab for their encouragement and support along the way. Finally, I would like to thank all the participants in the user study. This accomplishment would not have been possible without them.

ABSTRACT OF THE THESIS

Design of a Portable Shape Display for Augmented Reality

by

Tse Tsui

Master of Science in Engineering Sciences (Mechanical Engineering)

University of California San Diego, 2020

Professor Tania Morimoto, Chair

Augmented reality (AR) supplements the real environment with virtual objects, offering an immersive mode of interaction with potential for impact in a variety of applications. Recent advancements have included the ability to use one's phone as an AR display, which opens the possibility of more wide-spread adoption. Despite improvements in tracking and image processing, mobile augmented reality remains limited in its interactions, largely relying on button presses on a screen. To improve the immersiveness of AR environments and the richness of interactions, we propose a portable shape display and associated Unity App that enables users to feel the virtual objects being rendered on their phones. The device consists of a 3 x 3 array of pins, covered with a layer of soft foam to help make surfaces feel more continuous. A user

study is performed to evaluate the effect of important design parameters on the degree to which interactions with various objects are perceived as realistic. Based on the results of this initial study, a final device is fabricated and tested in a second user study aimed at determining the effectiveness of the device at conveying shape information. Without visual feedback, participants correctly identified a set of four shapes with 42.86% accuracy, demonstrating the potential of the device to be used in conjunction with AR apps, including for education and design.

Chapter 1

Introduction

Virtual reality (VR) and augmented reality (AR) offer a more immersive experience compared to traditional computing methods. Augmented reality, in particular, has the potential to improve even routine activities by supplementing the real world with virtual objects, which can enhance the information available in real-time [4]. From the earliest Head-Worn Display (HWD) in 1960s, to current commercial devices such as the Microsoft HoloLens headset, AR devices are becoming increasingly available to the public. Applications such as manufacturing, maintenance, training, and surgery show potential for improved efficiency, reduced errors, improved safety, and lower costs [53] [66] [11]. The ubiquity of hardware, such as smartphones and tablets, along with advancements in their computing power, has led to the expansion and increased popularity of mobile AR applications [19]. For instance, mobile AR applications allow tourists to explore the world with new interactive experiences. Students could also benefit from AR technology by enhancing learning achievement, motivation, and performance in educational settings [39] [1]. Despite the increase in popularity of AR devices, feedback has remained largely limited to visual feedback [5].

Haptic feedback has the potential to enhance interactions in virtual environments[47]. A haptic device is a device relating to the sense of touch, including forces and torques sensed by muscles and joints, or pressure, shear, and vibration sensed by mechanoreceptors in our skin. Work to date has included a variety of devices, such as grounded haptic devices using

kinesthetic force feedback and ungrounded haptic devices with skin-deformation or vibrotactile haptic interface [22]. Encountered-type haptic displays represent another class of devices, which the user can directly explore, rather than relying on intermediate tools. Shape displays, created using an array of actuated pins, are one such promising encountered-type device [2], and have been created using a range of actuators, including linear actuators, shape-memory alloys, and hydraulics [41]. Although the size, actuation mechanism, and use-case varies, the majority remain limited to displaying objects in only “2.5-D”, since the 2-D array is constrained to remain in the plane of the table on which it sits [41]. In this work, we propose to enable a new mode of interaction by developing a portable shape display that can be used to feel 3-D objects over an unlimited workspace.

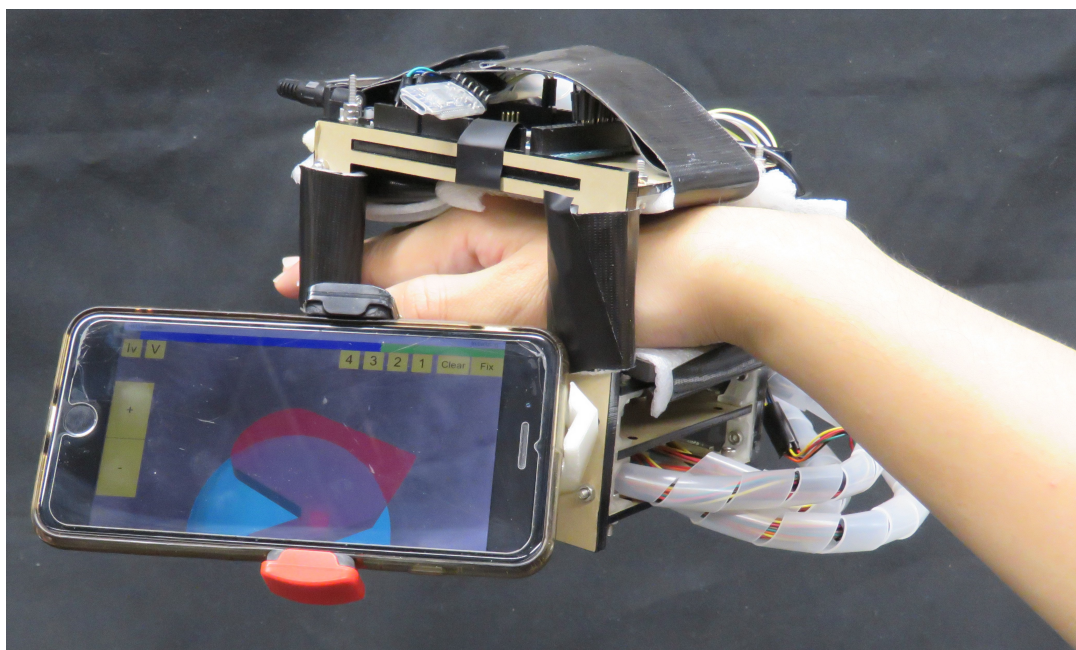


Figure 1.1. Device overview including portable shape display and integrated phone mount. A custom Unity App displays virtual objects as the user explores the augmented reality (AR) environment.

1.1 Grounded Haptic Devices

Kinesthetic devices are one of the most common type of haptic interface. These devices apply force to guide or inhibit the user's movement, and can connect the user to an AR environment. In order to apply relevant forces to the user, most kinesthetic devices are grounded, and the base remain stationary on a table or other surface as the user interacts with the tool or end-effector position of the devices. One example is the Geomagic Touch, also known as the Phantom Omni, which can provide stiffness and textures of virtual objects as well as free local space exploration. This device is capable of six degree-of-freedom movement and three degree-of-freedom force feedback [46]. The relationship between Geomagic Touch's virtual proxy coordinates and the global coordinates for all of the virtual graphic objects needs to be synchronized to achieve appropriate interaction [64] [50]. Despite the improvements in position accuracy, calibration errors and latency, the need for a fixed position of the grounded kinesthetic device, along with the need for external headsets or tracking systems, make practical implementation challenging [44][7].

Another category of grounded haptic devices in augmented reality includes body-grounded kinesthetic devices. This kind of haptic device is attached to the human body, most often the hand. The body is then used as a ground to absorb the reaction force during interaction [52]. Devices, such as exoskeletons and haptic gloves, are a common form in this field. Various actuators like classical DC motors, artificial muscles, pneumatic actuator, shape memory alloys and dielectric elastomers have been used to achieve light weight, low cost and strong grasping force feedback [54]. A few designs, such as DESR, Grability and Wolverine, simulate kinesthetic pad opposition grip force between fingers [69] [17] [18]. Previous designs on haptic gloves, such as RMII-ND, WHIPFI, MR gloves and soft robotic glove, transmit force from the fingers to the backside of the hand or wrist through linkages [12] [27] [9] [35]. There are also many commercial haptic gloves, such as CyberGrasp, HaptX and VRgluv, available to the public. Most applications for body-grounded kinesthetic devices, however, are in virtual reality, rather

than in augmented reality. Since these devices do not need to be fixed in one location, these devices are more portable with cables and transmitting lines connecting to the actuators. One challenge to this being portable, is that it is harder to synchronize with image displays in the AR environment. Devices using a headset to track their location, need to be kept in the sight of the sensor or the camera to render the haptic feedback [65] [3] [14]. Current research focuses on the measurement of accurate hand gestures and positions for future cooperation between body-grounded kinesthetic devices and image displays in AR environments [52].

1.2 Ungrounded Haptic Devices

In addition to the grounded haptic devices using kinesthetic force feedback, a large area of research includes ungrounded haptic devices. Instead of direct kinesthetic force feedback, some of these devices provide cutaneous feedback often via haptic illusions. They can be more comfortable and lightweight for use in AR environments. Three main types of devices including skin deformation devices and vibrotactile devices, which each stimulate the mechanoreceptors in the skin to generate artificial human sensations, and mid-air devices, which use ultrasound to generate the shape of objects or air flow to generate force feedback.

Skin deformation devices, providing cutaneous force feedback, can display multi-DoF shear or normal force to our skin [56] [28]. Devices using lightweight and inexpensive belt-driven mechanisms, such as hRing, W-FYD and Altered Touch, provide normal and stretch stimuli on the finger and can create a sense of volume, stiffness and weight of virtual objects [51] [8] [49]. Other type of devices driven by servos or DC motors with linkages, such as LinkTouch, 3-RSR and 3-RRS, press mobile platforms on the fingerpad to provide translational skin deformation and simulate contacts with virtual surfaces. [63] [42] [15][58]. Both belt-driven and linkage designs have similar results to improve the performance and illusion during specific tasks in AR environments [45]. Other devices using different mechanisms, including a rolling sphere, skin-stretch for the upper limb, and forearm linkages have also been explored for

creating skin deformation haptic feedback [68] [16] [48].

Vibrotactile devices use actuators, such as small linear resonant actuators, voice coils, or speakers, to generate vibration for interaction cues, illusions of surface texture, or sensations of force. By controlling the pulse width and delay of a sequence of actuators, we can provide a sense of direction cues and continuous lateral motion with different frequency, intensity and velocity [37] [21] [33]. Compared to kinesthetic devices, vibrotactile devices have high enough bandwidth to generate high-frequency vibrations for modeling surface texture. Devices using electrovibration effects can generate signal waves to render different surface textures [5]. The sense of roughness and friction when interacting with a physical object can be presented using voice coils and solenoids [20]. It is also possible to generate a sensation of pulling force or simulate weight of virtual objects with vibration feedback [23] [24] [17]. Midair devices are another class of ungrounded haptic devices that provide free space and lightweight interaction. The 3D shape of virtual objects can be felt using focused ultrasound or air vortex without the need to contact the actuators [43] [32] [60]. Force feedback can also be generated with air jets or propellers [57] [31].

Similar to body-grounded haptic devices, most of the ungrounded haptic devices in augmented reality face the challenge of syncing location of devices and images. Many tracking systems, such as the ARToolKit gesture tracking system, AR headset, and 180 magnetic tracking sensor, have been used to locate the ungrounded haptic devices [13] [49] [58]. For many skin deformation devices and vibrotactile devices, the haptic feedback can only generate the illusion of sensation instead of solid touch like grounded haptic devices. For Midair devices, most designs are not portable due to the need to place actuators, including ultrasonic array and air pump, on the ground.

1.3 Encountered Type Haptic Display

With the benefit of free exploration and an actual solid surface, encountered type haptic displays provide convincing sensations compared to body-grounded kinesthetic devices [54]. Shape displays are one category of these devices that often uses a 2-D pin array to render the contour of a virtual object. These displays are considered to have “2.5-D” because they render the shape of 3-D objects with a grounded 2-D pin array, making it impossible to render a true 3-D shape [41]. Previous designs range from large-scale pin array displays, including FEELEX and inFORM, to fingertip shape displays, such as PinPad [34] [25] [38]. A variety of difference actuators, including DC motors with lead screws, rotational servos with linkages, pneumatic actuators, and shape memory alloy have been used to move the pin array to render shapes [30] [61] [67]. Different device designs, such as having a small pin array on the fingertips or mobile devices, and changing the shape of airbags in the hand, enable a true 3D shape display [29] [6] [36] [62]. The challenge of applying encountered type haptic devices to virtual environments also lies in the restriction of the workspace with external cameras or tracking systems and the weight of sensors or actuators [59].

1.4 Contributions

The contributions of this work are as follows. (1) We propose a shape display (Fig. 1.1) that enables true 3-D interactions, where the user can approach and feel the virtual objects from any direction. This type of interaction differs from that of previous shape displays, which are typically 2.5-D. (2) We propose a device design that enables an unlimited workspace and is compatible with mobile AR, since it is not tethered or grounded and can be worn by the user, while simultaneously viewing the AR environment. (3) We present a preliminary study demonstrating users’ ability to identify virtual objects using the rendered shape information alone, with no visual feedback, demonstrating its potential as a haptic feedback device for interactions in AR.

Chapter 2

System Design

In this section, we present the design of a portable haptic device that renders the shape of AR objects using a pin array covered with a soft material, along with a customizable Unity App. The design objectives of this device focus on creating a solid shape display, an unlimited workspace, and a portable and open-source devices. First, the actuating system needs to provide sufficient power to support at least the weight of the human hand. Second, an unlimited workspace would enable users to explore the AR environment freely without the restriction from the device or the system. To achieve this, the system itself should be able to synchronize the image display of the AR environment and shape display haptic feedback without the need for an external tracking system. Third, to create a portable design, the device must be lightweight and have a small footprint. Portability enables outdoor AR interaction, allowing users to experience more immersive AR interactions combined with daily life [55]. Finally, accessibility for the public to the hardware and software designs could provide the opportunity to accelerate the research and development for application in AR.

2.1 Hardware Design

To achieve a portable design, we aim to create a small volume and light weight device. The portable AR shape display, shown in Fig. 2.1, consists of a 9 pin assembly arranged in a 3x3 grid. The dimensions and exploded view are shown in Fig. 2.2. A main base frame, made from

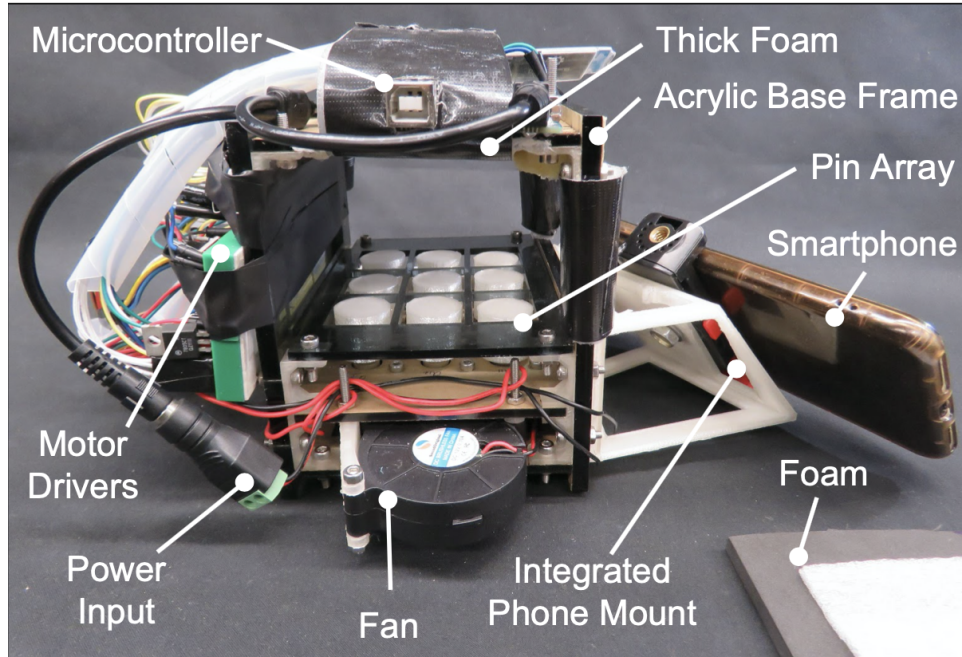


Figure 2.1. The proposed device uses a pin array covered with a soft material (shown on the side for ease-of-viewing) to display the shape of AR objects. A smartphone installed with a custom Unity App is used to track the motion of the device and to compute the parameters used to render the proper shape.

acrylic, is designed to support this pin array, as well as create a space for the user’s hand to slip inside. The dimensions of the device were selected to accommodate most adult hand sizes [26], the phone size and location of the camera, and the linear actuator size. With the knowledge of average human hand size, the space for the hand to slip inside is determined (130 mm x 100 mm x 60 mm). A thick polyethylene foam is added on the top of the space to fit the back of the user’s hand. It can increase user comfort and, when the user raises the device, still reserves a uniform height of about 10 mm between palm and the pin array for displaying the shape.

The pin array has a total weight of 225 g and a sufficient number of pins to display the contour of a sphere AR object in 100 mm diameter. To make the displayed shapes appear more continuous, and to increase user comfort, a 3.175 mm thin layer of polyethylene foam is placed over the pins, shown on the bottom right corner in Fig. 2.1. A fan is also attached to the base frame to cool the linear actuators. The pin assemblies, shown in Fig.2.3a, each consists of a

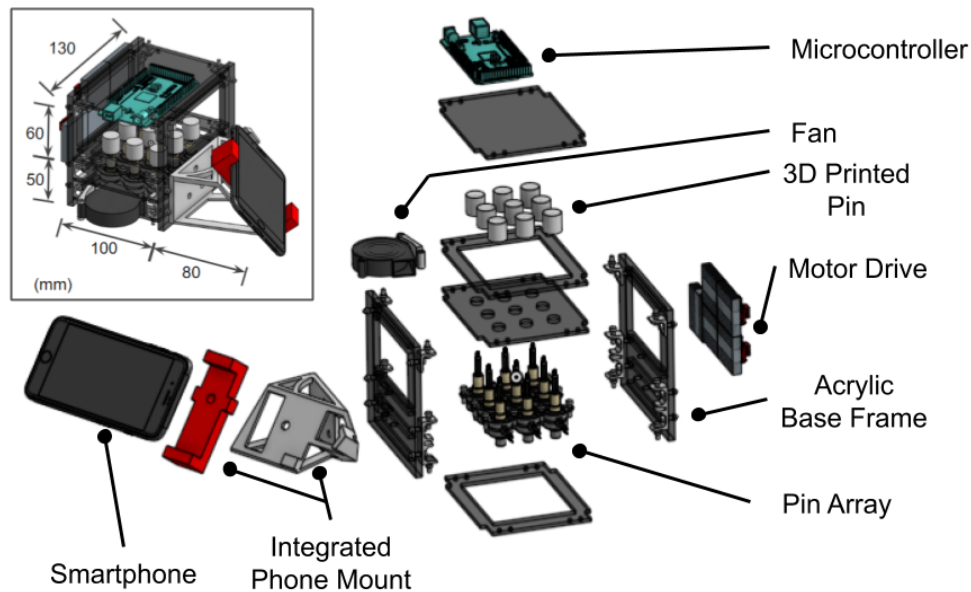


Figure 2.2. The dimensions and the exploded view of the device are shown here. The approximate volume and weight of the device, with an iPhone 7 plus attached, are $2.2 \times 10^6 \text{ mm}^3$ (2.2 L) and 1.2 kg. The device can be assembled with 3D printed connector with M3 screws and nuts.

Portescap 20DAM10-K linear actuator and the pin itself, which is fabricated out of PLA and is designed to easily be attached and removed. The linear actuator with 20 mm diameter weighs 25 g and costs about 40 dollars. It can provide 15 mm maximum stroke length and 8 N force output at 10 mm/s maximum speed, which is strong enough to support a human hand with a weight of 0.6 kg ($\sim 6 \text{ N}$). The linear actuator is selected due to its compact design. The actuator consists of a bipolar stepper motor with a built-in lead screw, which can achieve translational motion without the need for external mechanical components, such as a lead screw, linear slide, or linkages, which many shape display devices use. The last critical hardware component is an integrated phone mount that is needed to maintain the relative position of the smartphone and the base frame to ensure proper rendering of the haptic feedback. The phone mount has a window for the camera to maintain a clear field-of-view for sensing and rendering the AR environments.

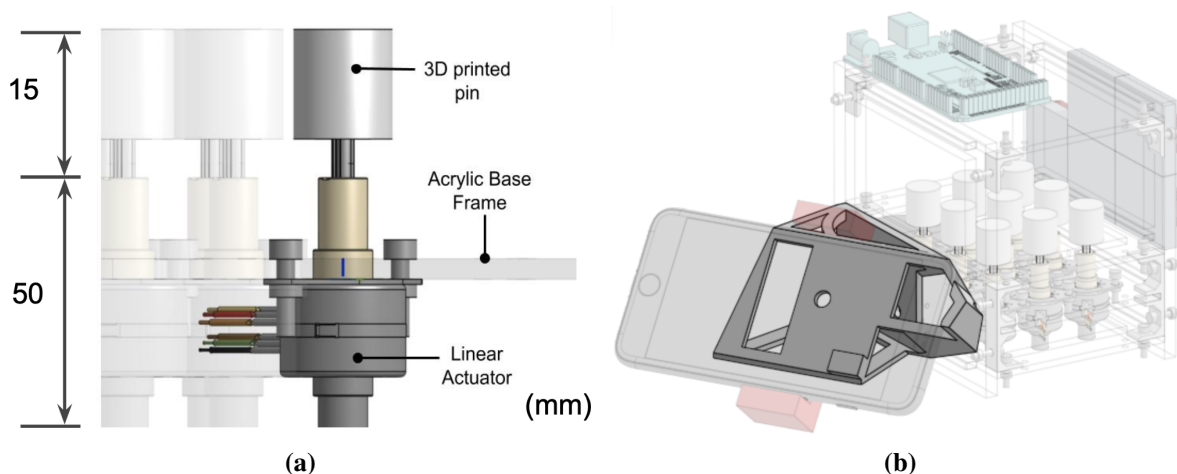


Figure 2.3. (a) Each pin assembly in the array mounts to the base frame and consists of a removable 3D printed pin that attaches to the top of a linear actuator.(b) The integrated phone mount provides a window for smartphone cameras to render the AR environments without being blocked by the acrylic base frame.

2.2 Software and Electronics

In this thesis, we developed a Unity App that visually displays the AR objects, as well as computes the parameters needed to render the haptic effects. The shape rendering method is discussed in Chapter 2.3. We use an iPhone 7 plus, since it supports an AR library called ARKit, which can combine device motion tracking and camera scene capture. Using this AR library, all interactions begin with placing an AR object on a flat surface. These AR objects can either be premade or can be objects that have been designed by the user. Information from the dual cameras and motion sensor are then used to track the motions of the smartphone, render the virtual objects, and compute the desired height of each pin in the array. This height data is then sent via Bluetooth to the control unit, which consists of a micro control unit (Arduino Mega) and a Bluetooth Low Energy module (HM-10) (see Fig. 2.4). The height information is converted into the desired displacement of the 9 linear actuators, which are driven using Allegro A4988 stepper motor drivers. We use an AC adaptor as a DC 12V 1A power source, but can easily switch to a portable battery in future versions to enable truly unlimited workspace.

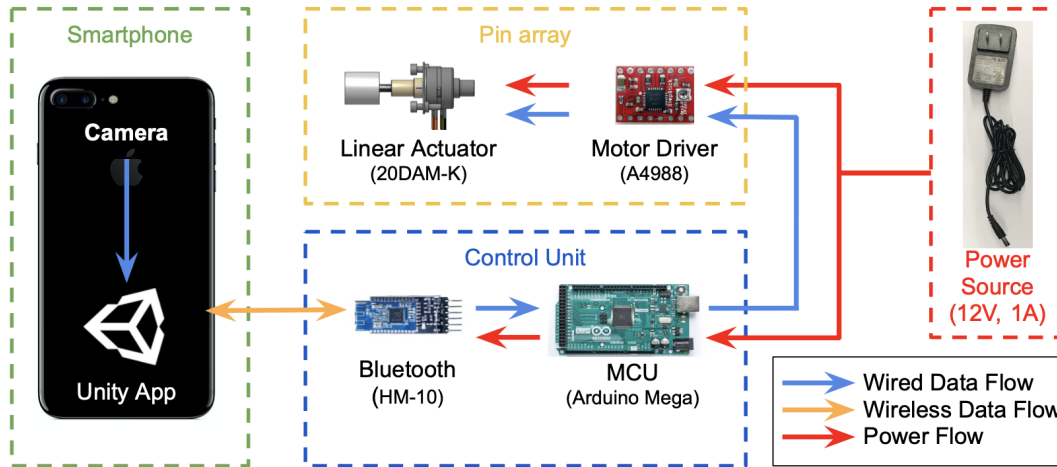


Figure 2.4. Block diagram of the signal flows for the proposed system. Information about the height of the device relative to the AR objects is captured using the dual cameras and processed in the Unity App. This information is sent via Bluetooth to the MCU and used to control the heights of the pins in order to display the desired shape.

2.3 Shape Rendering Method

In order to determine the heights of the pins needed to render a desired shape, the distance between the linear actuator and the surface of the AR objects must be computed. In our Unity App, we developed a ray-casting script that uses the camera on the phone to detect the motion of the device and subsequently calculate the height of the collision between each linear actuator and the surface of the AR object. As shown in Fig. 2.5, the red hand-shape is used as a virtual proxy, representing the area felt by the user, and the white casting lines are the rays that start 200 mm above the proxy and end at the bottom of it. Both the user proxy and the casting lines move with the device, but only the proxy is visible to the user.

When the proxy moves inside the AR objects, the casting lines are used to determine this penetration distance, which is equal to the total length of the casting line minus the distance between the starting point of the ray and the point of contact between the ray and the surface of the virtual object. This height data, which is proportional to the desired height of the pin, and therefore the distance that the linear actuator needs to move, is then sent via bluetooth to the

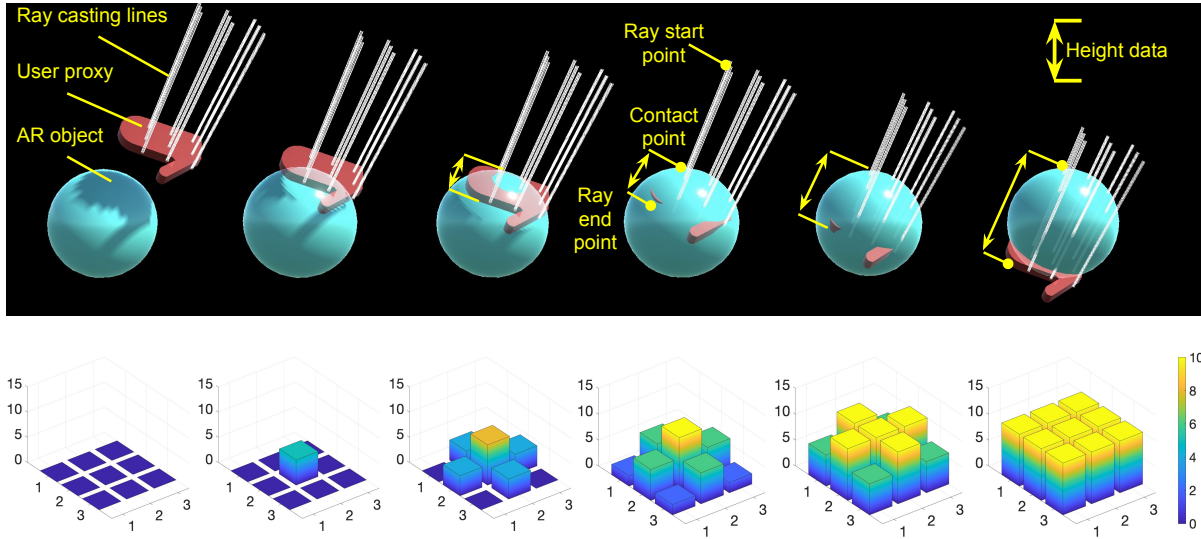


Figure 2.5. Method for rendering the shape of a virtual sphere as (from left to right) the red hand-shape user proxy moves into the virtual blue sphere. A ray-casting script calculates height of the collision between each linear actuator and the surface of the AR object. A simulation of the shape display corresponding to this interaction is shown as a time-series below.

MCU.

There are two main factors contributing to the effectiveness of the shape rendering– the maximum speed and the maximum stroke length of the linear actuators. Because the actuators are controlled in such a way that the entire display is refreshed at once, the maximum speed of the actuator, along with the distance the actuator needs to travel, determines the refresh rate. For example, traveling through the worst case scenario of the maximum stroke length (15 mm) takes 2.2 seconds at its 10 mm/s maximum speed, while it only takes 0.07 second to travel 1 mm. It should be noted that to avoid noticeable delays between each refresh, the user should limit his or her speed of exploration to the maximum speed of the actuators, if moving continuously. Since this is slower than typically comfortable for human movement, an alternative is to pause between large movements. Selecting actuators with higher maximum speeds would help improve the refresh rates of future versions. Since the actuators are limited by their stroke length, if the proxy moves too far beneath the surface of the AR object, the device will saturate and the object will render as a flat surface (see last image in Fig. 2.5). To avoid this saturation and help convey

to the user that they have pushed too far into the virtual object, a pushing force is simulated by commanding all actuators to move 1 mm at maximum speed if any actuator comes within 5 mm of its maximum stroke length. The purpose is to try to convey to the user that they have hit a boundary and should move back out. Another option is to allow users to move the position of AR objects when penetrating the surface with more than a given value. This situation is mostly important for the user studies where the virtual objects are not visually displayed to the user. In real use-cases with visual feedback, we do not anticipate this issue.

Chapter 3

Device Parameter User Study

In this study, we aimed to determine whether the size, shape, or contact stiffness of the pin array affects user's interaction with virtual objects. There were three main research questions we looked to answer. The first question was whether there is a correlation between hand size and preferred pin size. In other words, do users with a similar hand size prefer a similar pin size? The second question was whether specific pin shapes are more suitable for rendering particular objects. The final question was whether softer contact foam covering the pin array could help to improve object rendering. With better knowledge of these parameters, we can determine whether there is a need to have a customized setup for users, and which device parameters will enable more realistic object rendering.

To evaluate the effects of various device parameters, 15 right-handed participants took part in the three experiments described in this section. Participants were 20-34 years old and there were 8 males and 7 females. Eight of the participants had prior experience with VR/AR devices, and twelve had prior experience interacting with haptic devices. The proximal interphalangeal joint (PIJ) breadth (equivalent to the width of the middle finger at the knuckle) and the hand breadth were measured for each participant at the start of their session [26]. Based on the PIJ breadth value, participants were split into one of two subgroups, since we hypothesized that users with different hand sizes would prefer a device with different pin sizes. Group 1 consisted of 7 subjects with a mean PIJ of 16.36 ± 1.15 mm, and Group 2 consisted of

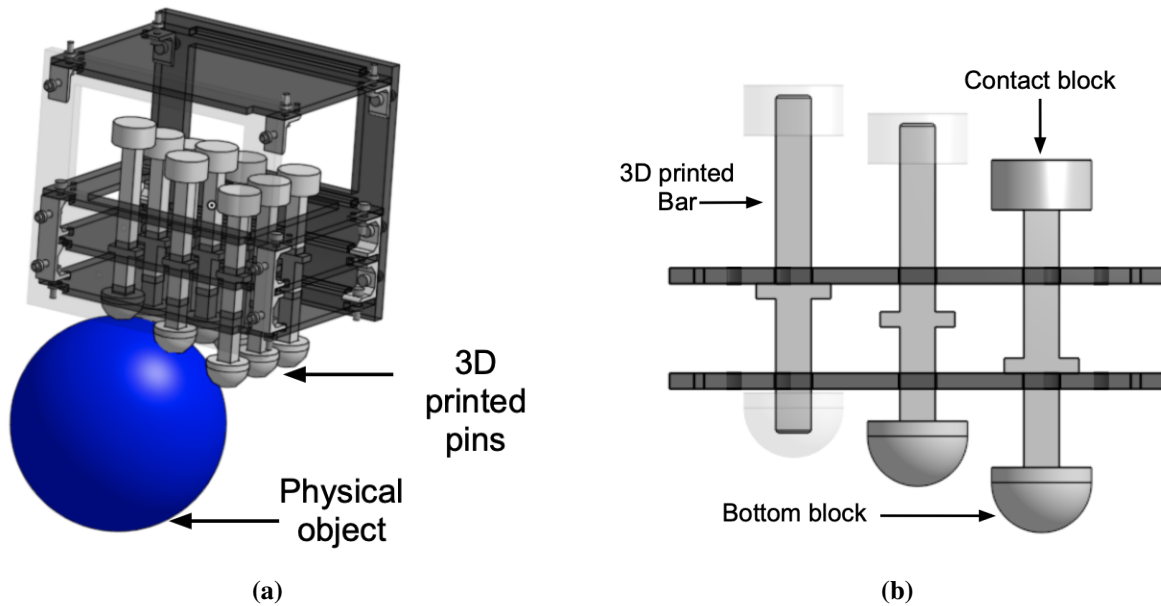


Figure 3.1. A simplified, non-mechatronic version of the device is used to determine device design parameters. (a) The actuators are replaced with 3D printed pin assemblies that can directly reflect the shape of a physical object (blue ball) located beneath the device. (b) Each 3D printed pin assembly consists of a contact block, a 3D printed bar and a bottom block.

8 subjects with a mean PIJ of 18.29 ± 0.68 mm. All participants provided written informed consent prior to the study in accordance with the UC San Diego Institutional Review Board.

3.1 Device Setup

Because the goal was to evaluate the effects of various mechanical parameters of the device, independent of the haptic rendering algorithm, a simplified, non-mechatronic version of the device was used (Fig.3.1). In this version of the device, the actuators were replaced with 3D printed pin assemblies that slide up and down based on interaction with an actual physical object, therefore directly reflecting the object's shape. The contact block is designed to easily be swapped depend on the parameters needed for each experiment. The 3D printed bar is designed to limit the maximum displacement of 3D printed pin assembly to be the same as maximum stroke length of the linear actuator, which is 15 mm. The bottom block is designed in a semi-sphere shape to smoothly scratch through the object's shape. A thin (3.175 mm) polyethylene

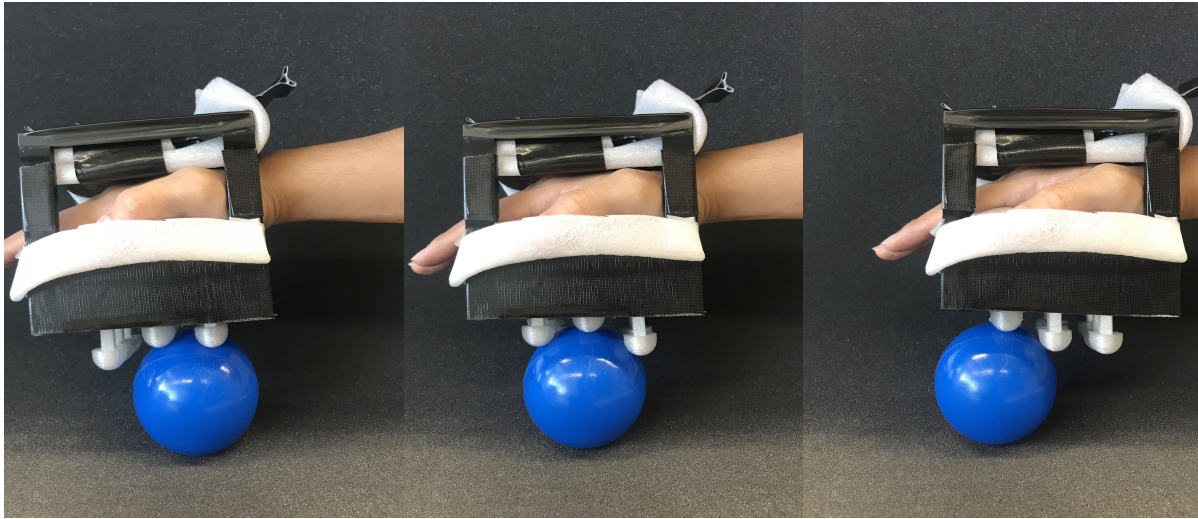


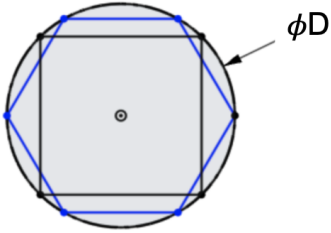

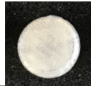

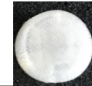

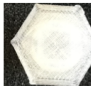

Figure 3.2. Example of user interaction with an actual physical object when using the simplified device in the first user study.

foam was placed over the pins as a base layer. The adjustment the thick polyethylene foam, described in Chapter 2, was needed for each participants to ensure their hand was pressed on the 3D printed bars with comfortable and movable space of 10 mm for proper shape display.

3.2 Experimental Procedure

Before the study began, participants were given 5 minutes to practice using the simplified device to feel an actual sphere (76.52 mm in diameter), followed by a cuboid (150 mm x 128 mm x 74 mm). The study consisted of three experiments, with six trials each. For each experiment, participants used the simplified device with varying parameters to feel the same sphere and cuboid in 5 minutes. Each experiment was designed to measure a particular parameter shown in 3.1– pin size, pin shape, or contact foam stiffness- hypothesized to affect perception of the haptically rendered objects.

At the end of each trial, participants were asked to evaluate their level of agreement on a 7-point Likert scale (1 = strongly disagree, 7 = strongly agree) to the statement, “This interaction feels real”. For all experiments, a two-sided T-test with a significance value of 0.05 was used to determine whether there was a significant difference between any two independent

Design Parameters	A	B	C	D	Example of pins: (top view) 
Size(D) (mm)	13 	16 	18 	20 	
Shape	square 	hexagon 	circle 	NA	
Foam stiffness* (psi)	2-5	5-9	9-14	NA	

*Foam stiffness is represented as pressure to compress 25% of foam thickness.

Table 3.1. All of the parameters used in device parameters user study are shown in this table. One section of the study was designed for each of the 3 parameters. For each section, the other two parameters were the same and participants used 3 out of the 4 categories(A,B,C and D). Examples of pins are drawn on the right, where D is the diameter of pin size and all pin shapes are inscribed in a circle of diameter D.

groups of data.

3.3 Pin Size Experiment

3.3.1 Experimental Setup

The non-mechatronic version of the device was fitted with a set of pins that were either 13, 16, or 20 mm in diameter, shown in the row of design parameters “Size” of Table 3.1. The pins all had a circular cross section. No contact foam other than the base layer was used.

3.3.2 Results and Discussion

To determine whether hand size affects which pin size leads to a more realistic object interaction, the two subgroups, were compared. There was no statistically significant difference found for any pin size ($p=0.43, 0.73, 0.95$ and $p=0.41, 0.85, 0.31$ for the sphere and cube,

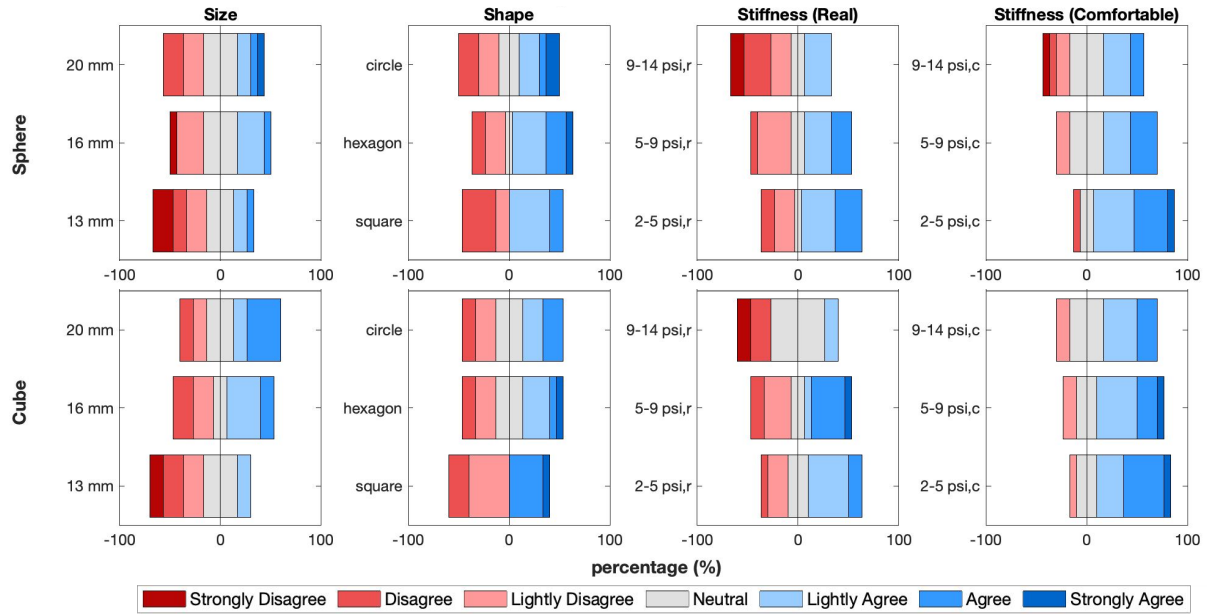


Figure 3.3. The data visualization of three experiments are shown here. The plots are created by centering around the neutral value (4 point) and plotting the data in a horizontally stacked percentage bar chart using MATLAB.

respectively). The data from these two groups was therefore combined for the remainder of the analysis in this pin-size study.

The visualization of combined data is shown in the first column of 3.3. As shown in Table 3.2, there was a statistically significant difference between the 13 mm and 20 mm pins for interactions with the sphere, where participants preferred the larger pin size. There was no statistically significant difference between pin sizes for interactions with the cube. The results showed that, contrary to the initial hypothesis, preference for pin size was not dependent on hand size as measured by the PIJ breadth. The remainder of the experiments in this chapter use different pin sizes based on hand size, however, the final device, described and tested in Chapter 4, uses a single pin size for all participants due to the results shown here. The larger (20 mm) pins are selected for that final device since the results showed that participants thought that interactions felt more realistic with these larger pins, at least when interacting with a spherical object. There was no obvious preference for a particular pin size when interacting with a cube-shaped object.

Table 3.2. Results from evaluating pin size, pin shape, and foam stiffness

	Pin Size [mm]			Pin Shape			Foam Stiffness [psi]			
	A	B	p-val	A	B	p-val	A	B	p-val	(comfort) p-val
Sphere	13	16	0.09	Circle	Hexagon	1.00	2-5	5-9	0.90	0.42
	13	20	0.01*	Circle	Square	0.91	2-5	9-14	0.04*	0.12
	16	20	0.45	Hexagon	Square	0.91	5-9	9-14	0.07	0.50
Cube	13	16	0.16	Circle	Hexagon	0.58	2-5	5-9	0.70	0.26
	13	20	0.24	Circle	Square	0.66	2-5	9-14	0.02*	0.03*
	16	20	0.89	Hexagon	Square	0.31	5-9	9-14	0.05*	0.19

*Significant difference between groups ($p < 0.05$)

3.4 Pin Shape Experiment

3.4.1 Experimental Setup

The non-mechatronic version of the device was fitted with pins of different shapes, including circular, hexagonal, and square, shown in the row of design parameters “Shape” of Table 3.1.. Dimensions of each shape were selected such that the shape was inscribed inside a circle of diameter D , where D was selected based on the user’s PIJ breadth. For participants in Group 1, $D = 16$ mm and for Group 2, $D = 18$ mm. No contact foam other than the base layer was used.

3.4.2 Results and Discussion

The visualization of data is shown in the second column of 3.3. As seen in Table 3.2, there was no statistically significant difference between any of the pin shapes for interactions with the sphere or the cube. It was therefore determined that the pin shape did not appear to be a crucial design parameter, at least in the context of perceived realism of objects, and a circular pin shape was selected for the final device design.

3.5 Contact Foam Stiffness Experiment

3.5.1 Experimental Setup

The non-mechatronic device was fitted with circular pins, whose size was again determined based on their hand-size group (16 mm diameter for Group 1 and 18 mm diameter for Group 2). Three different stiffness of neoprene foams, shown in the row of design parameters “Foam stiffness” of Table 3.1, were then placed below the thin base layer and users could again interact with the physical objects. All three foams had a thickness of 6.35 mm and the stiffness values, as reported by the manufacturer, were 2-5 psi, 5-9 psi, 9-14 psi, where stiffness was represented as the pressure to compress 25% of the thickness. Participants were asked to respond and evaluate their level of agreement on a 7-point Likert scale to an additional statement: “This interaction feels comfortable”.

3.5.2 Results and Discussion

The visualization of both real and comfortable data are shown in the third and fourth column of 3.3. For interactions with both the sphere and cube, there was a statistically significant difference between the reported realism using the softest (2-5 psi) and hardest (9-14 psi) foams, with the softer foam rated as feeling more realistic. In addition, for interactions with the cube, there was a statistically significant difference between the reported level of comfort between these same two materials, with a preference again towards the softer foam. The softest foam was selected for the final device.

Chapter 4

Object Identification User Study

As a result of the findings from the study described in Chapter 3, we fabricated a fully-functioning device with 20 mm diameter circular pins and 2-5 psi stiffness foam. All participants were asked to use this same device to interact with and identify various AR objects. The goal was to evaluate the effectiveness of the device in displaying shape information for augmented reality. Seven right-handed male participants took part in this final experiment. Participants were between 15-29 years old, and their mean PIJ breadth was 17.26 ± 0.78 mm. Two of the participants had prior experience with VR/AR devices, while the other five did not. All of the participants had prior experience interacting with haptic devices. All participants provided written informed consent prior to the study in accordance with the UC San Diego Institutional Review Board.

4.1 Experimental Procedure

The study consisted of 1 practice session, followed by 12 trials. During the practice session, participants were asked to do the same adjustment of the thick polyethylene foam for the proper shape display, described in Chapter 3.1, and use the device to interact with 2 different objects (an ellipsoid and a wedge), both with and without being able to visually see them. The objects were all surrounded by a cube frame that was designed to indicate the workspace in which to interact. During the actual study, a different set of objects was rendered inside this same

		Predicted Class				Sensitivity	Precision
		Cube	Cylinder	Pyramid	Sphere		
True Class	Cube	9	5	3	4	42.9%	47.4%
	Cylinder	6	7	1	7	33.3%	26.9%
	Pyramid		6	11	4	52.4%	73.3%
	Sphere	4	8		9	42.9%	37.5%

Figure 4.1. Confusion matrix showing true rendered shape versus predicted shapes.

frame, however, the objects themselves were not visually displayed. For each trial, participants interacted with a single virtual object and were asked to identify which of the four objects (sphere, cylinder, cube, or pyramid) they felt, as well as their level of confidence (on a 5-point Likert scale) in their selection, where 1 meant “not at all confident” and 5 meant “extremely confident”.

4.2 Results

Results from the experiment can be seen in the confusion matrix in Fig. 4.1. Participants were successful in identifying the correct shape of the virtual objects with 42.86% accuracy, and, given a maximum of 90 seconds per trial to interact with the virtual object, participants responded in an average of 76.79 ± 17.7 seconds. There was no statistically significant difference between correctly and incorrectly identified virtual objects for either the time or confidence level (shown in Table 4.1.) Sensitivity and precision values were also calculated for each of the objects. The pyramid had the highest sensitivity value, meaning that it had the highest rate of being correctly identified when it was presented. It also had the highest precision value, meaning that it had the highest probability of being correctly identified among all shapes identified as a pyramid. These results indicate that features such as the peak of the pyramid may be easier to distinguish when no visual feedback is present. Qualitative feedback from participants seem to match this analysis, since many reported a strategy of first locating any corner-like sensations in the environment. Although the precision value for the cube was slightly higher than that for the sphere, their sensitivity values were equal, generally indicating the difficulty in distinguishing

Table 4.1. Results from evaluating time and confidence level.

Average	Total	Correct	Incorrect	p-val
Time(s)	76.80 ± 17.70	75.54±18.17	77.5±17.62	0.61
Confidence level	3.05±1.18	3.30±1.21	2.85±1.13	0.083

between a curved surface and a flat surface with edges when no visual feedback is given. The most likely explanation is that the lack of visual feedback means it is easier to penetrate too far beneath the surface of the virtual object, causing the device to saturate and render a flat surface as shown previously in Fig. 2.5. The cylinder proved the most difficult to identify, likely due to its combination of both flat and curved surfaces, as well as curved edges. The limitation of this user study lies in the speed limit and weight of the device. The speed limit of 10 mm/s restricts user's movement and 1.2 kg weight of the device could cause fatigue to the user after a continuous 10 minutes of usage. Therefore, the practice section, time limit, and resting time for these experiments is needed.

Chapter 5

Preliminary Application

Applications of AR devices range from selfies, gaming, and art, to navigation, education, and manufacturing. In this chapter, we present two preliminary applications for the device. The first application is a beating heart object that can demonstrate a dynamic surface motion. The second application is an mass-spring-damper (MSD) system that demonstrates the movement of a cuboid mass can be affected by changing the spring and damping coefficients. Using a similar approach, many other applications can be developed for the portable shape display.

5.1 Dynamic Surface Demonstration

Examining a virtual 3D heart through an AR headset may be helpful to learn the structure of heart. Feeling the cardiac cycle through AR devices, on the other hand, can provide more information than visual feedback alone. In Fig.5.1a, we create a beating heart model to demonstrate the ability of the device to render a dynamic surface. The cardiac cycle animation and mesh of the beating heart model, shown in Fig.5.1b and Fig.5.1c, is purchased from the Unity asset store. In the Unity App, the device displays the shape of the heart when contacting the surface of the mesh grid. Rather than modifying the mesh grid to adapt in size based on the beating motion, we simplified the simulation by adding four ellipsoids representing the four chamber of the heart (Fig.5.1d to Fig.5.1g). When each chamber of the heart expands or contracts in the animation, the corresponding ellipsoid expands or contracts as well, while the

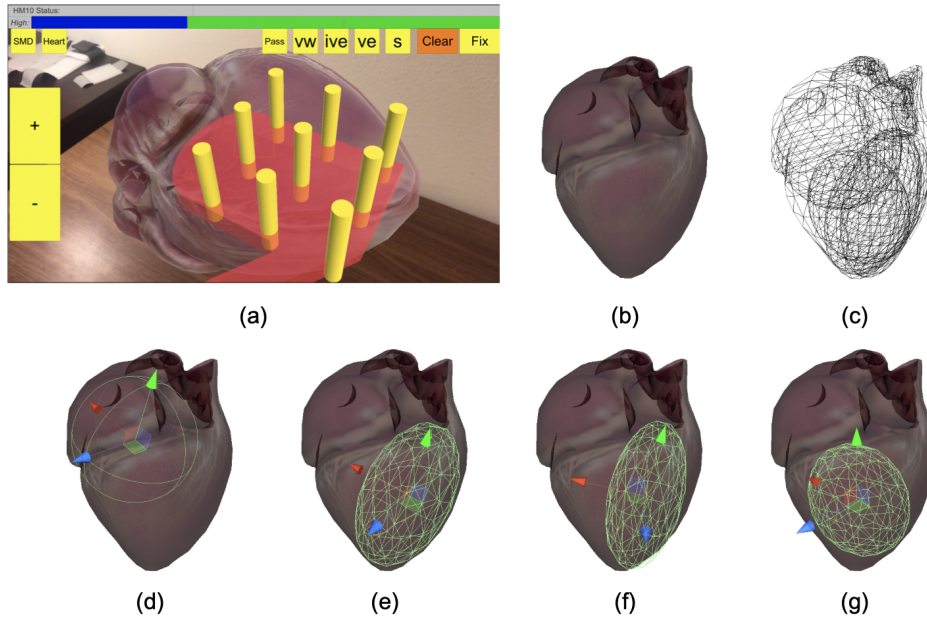


Figure 5.1. (a) In the Unity App, a virtual beating heart is placed on the table for the user to feel the heartbeat in contact with the surface of AR environment. (b) and (c) The virtual beating heart model has mesh grid for rendering virtual object surface. (d) to (g) Four ellipsoid virtual objects are created to provide surface motion that move with animation.

original mesh grid remains static. Other than adding four ellipsoids and synchronizing their movement to the cardiac cycle animation, no additional software is needed compared to the original setup. The size of beating heart, the speed of animation and the amount of the ellipsoids can be customized to generate more genuine surface motion. The fastest heart beat depends on the maximum speed that the device can render, which is currently 10 mm/s. Many possible scenarios of dynamic surface motion can be designed including, for example, a ripple on the surface of water and the shaking of an old engine that needs to be repaired. With these types of applications, the device can provide more immersive experiences in AR environments.

5.2 Mass Spring Damper Demonstration

In Fig.5.2(a), We create a mass-spring-damper system to demonstrate the ability of the shape display to render a physical simulation, with varying system parameters, to the user. A blue virtual cube, as shown in Fig.5.2(b), with a weight of 1 kg, is connected to a fixed point

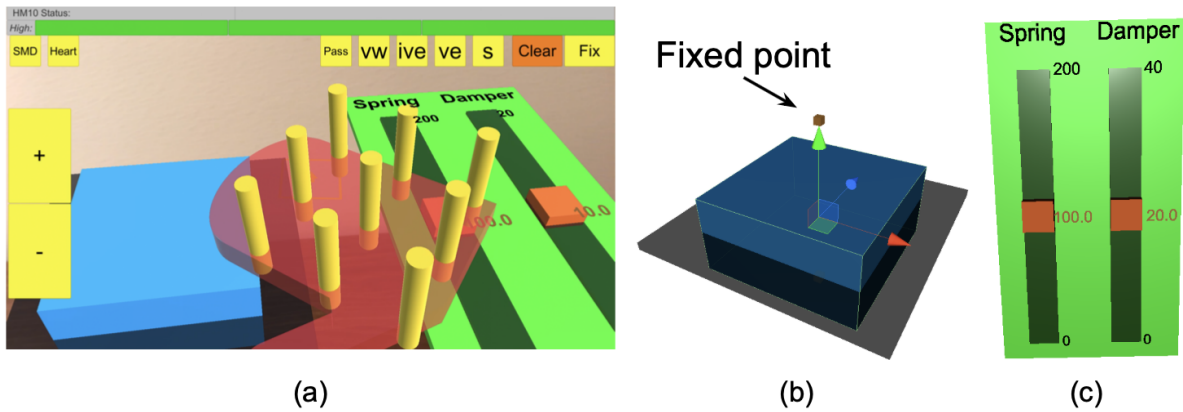


Figure 5.2. (a) In the Unity App, A MSD system is created to demonstrate a physical simulation with changeable spring and damping coefficient. (b) A 1kg virtual cube is connected to a fixed point with a virtual spring and damper. (c) A panel is used to change spring and damping coefficient in real time. User can feel the shape of cube slider when changing the coefficient of the MSD system.

above a black plane, which indicates the equilibrium position of the blue virtual cube under default parameters, with a transparent virtual spring and damper. A green virtual panel, as shown in Fig.5.2(c), with two slider bars show the minimum, current, and maximum values of spring and damper coefficients for the MSD system. During the interaction, user can move the orange slider to change both of the coefficient and, therefore, change the feeling when pressing on the blue virtual cube with the portable shape display device. The difference in speed and oscillation of the blue virtual cube motion can be felt. The user can also feel the shape of the orange slider to make it easier to interact with. An extra Unity script is needed to change both of the coefficients in real time. The speed limitation of this application is similar to the previous dynamic surface demonstration. If the blue virtual cube oscillates faster than 10 mm/s, the rendering shape will not coordinate with the image display. The benefit of this application is that user can feel the physical simulation under changing parameters, which could potentially help them better understand the dynamics of physical world.

Chapter 6

Conclusions and Future Work

In this work, we present a portable shape display for interacting with 3-D objects in augmented reality. A user study is performed to determine the effects of important design parameters, including pin size, pin shape, and foam stiffness, on the perceived realism of interactions with virtual objects. The responses were evaluated on a 7-point Likert scale and analyzed using a two-sided T-test with a significance value of 0.05. The results show a preference with a statistically significant difference for a pin size of 20 mm over 13 mm and foam stiffness of 2-5 psi over 9-14 psi. A final device, using parameters based on the results of device parameters user study, is then fabricated and tested to evaluate users' ability to identify different objects using only the rendered shape information without visual feedback. At the end of this thesis, we present two possible demonstrations for the preliminary application of this device. In the dynamic surface demonstration, a beating heart is presented to simulate the effect of a moving surface. In the mass-spring-damper demonstration, a cuboid MSD system is presented to test the of this device during interaction in the AR environments.

In the future, the device design, parameters, and performance, can be improved with further studies. For the hardware design of the device, the motor can be changed to a faster version (still with sufficient holding torque) to reduce the time delay during exploration. Multiple or a more sophisticated microcontroller can also be used to allow faster user movement when rendering a shape. The power input can be replaced by a battery to enable truly unlimited

workspace. Besides the adjustment to the equipment, the weight of the device can be significantly reduced by moving all of the control unit and the pin array to user's arm or body without restricting of interaction in the AR environments. Cooperation between multiple devices is also possible to provide new interactions among users. For the software design of the device, the Arduino and Unity programs can be improved to change the sampling time for rendering the shape based on the user's moving velocity. The current design only passively displays the shape of encountered AR objects. It is possible to interact with AR objects by adding a pressure sensor on the top of each pin assembly to sense the hand gesture of the user as the feedback signal. Combination with other haptic devices, such as adding vibration feedback on the pin array, is also possible to provide richer feedback[10].

To better understand the effects between device setup and realistic feelings for the user, more user studies can be performed by including a wider range of setting for the device parameters. For example, different number, height, or arrangement of the pin array, and different sizes of AR objects could be tuned to reach a higher resolution or comfort level [40]. The device performance can be evaluated in more realistic use-case scenarios that include visual feedback, and features can be added to enable manipulation of the objects as well. Existing applications in AR that include mostly visual and tactile feedback, such as drawing 3D solid objects in the air, changing terrain with a handheld controller and assembling a structure, could be improve by this device. It is also possible for students, designers, tourists and people in industry to benefit from learning, creating art, exploring, and solving technical problems through the interacting with this portable shape display.

Bibliography

- [1] Murat Akçayır and Gökçe Akçayır. Advantages and challenges associated with augmented reality for education: A systematic review of the literature. *Educational Research Review*, 20:1–11, 2017.
- [2] Jason Alexander, Anne Roudaut, Jürgen Steimle, Kasper Hornbæk, Miguel Bruns Alonso, Sean Follmer, and Timothy Merritt. Grand challenges in shape-changing interface research. In *Proceedings of the 2018 CHI Conference on Human Factors in Computing Systems*, pages 1–14, 2018.
- [3] L Almeida, E Lopes, B Yalçinkaya, R Martins, A Lopes, P Menezes, and G Pires. Towards natural interaction in immersive reality with a cyber-glove. In *2019 IEEE International Conference on Systems, Man and Cybernetics (SMC)*, pages 2653–2658. IEEE, 2019.
- [4] Ronald Azuma, Yohan Baillot, Reinhold Behringer, Steven Feiner, Simon Julier, and Blair MacIntyre. Recent advances in augmented reality. *IEEE computer graphics and applications*, 21(6):34–47, 2001.
- [5] Olivier Bau and Ivan Poupyrev. Revel: tactile feedback technology for augmented reality. *ACM Transactions on Graphics (TOG)*, 31(4):1–11, 2012.
- [6] Hrvoje Benko, Christian Holz, Mike Sinclair, and Eyal Ofek. Normaltouch and texture-touch: High-fidelity 3d haptic shape rendering on handheld virtual reality controllers. In *Proceedings of the 29th Annual Symposium on User Interface Software and Technology*, pages 717–728, 2016.
- [7] Gerald Bianchi, Benjamin Knoerlein, Gabor Szekely, and Matthias Harders. High precision augmented reality haptics. In *Proc. EuroHaptics*, volume 6, pages 169–178. Citeseer, 2006.
- [8] Matteo Bianchi, Edoardo Battaglia, Mattia Poggiani, Simone Ciotti, and Antonio Bicchi. A wearable fabric-based display for haptic multi-cue delivery. In *2016 IEEE haptics symposium (HAPTICS)*, pages 277–283. IEEE, 2016.
- [9] Jonathan Blake and Hakan B Gurocak. Haptic glove with mr brakes for virtual reality. *IEEE/ASME Transactions On Mechatronics*, 14(5):606–615, 2009.

- [10] Christoph W Borst and Charles D Cavanaugh. Haptic controller design and palm-sized vibrotactile array.
- [11] Eleonora Bottani and Giuseppe Vignali. Augmented reality technology in the manufacturing industry: A review of the last decade. *IISE Transactions*, 51(3):284–310, 2019.
- [12] Mourad Bouzit, Grigore Burdea, George Popescu, and Rares Boian. The rutgers master ii-new design force-feedback glove. *IEEE/ASME Transactions on mechatronics*, 7(2):256–263, 2002.
- [13] Volkert Buchmann, Stephen Violich, Mark Billinghurst, and Andy Cockburn. Fingartips: gesture based direct manipulation in augmented reality. In *Proceedings of the 2nd international conference on Computer graphics and interactive techniques in Australasia and South East Asia*, pages 212–221, 2004.
- [14] Siam Charoenseang and Sarut Panjan. 5-finger exoskeleton for assembly training in augmented reality. In *International Conference on Virtual and Mixed Reality*, pages 30–39. Springer, 2011.
- [15] Francesco Chinello, Monica Malvezzi, Claudio Pacchierotti, and Domenico Prattichizzo. Design and development of a 3rrs wearable fingertip cutaneous device. In *2015 IEEE International Conference on Advanced Intelligent Mechatronics (AIM)*, pages 293–298. IEEE, 2015.
- [16] Francesco Chinello, Claudio Pacchierotti, Nikos G Tsagarakis, and Domenico Prattichizzo. Design of a wearable skin stretch cutaneous device for the upper limb. In *2016 IEEE Haptics Symposium (HAPTICS)*, pages 14–20. IEEE, 2016.
- [17] Inrak Choi, Heather Culbertson, Mark R Miller, Alex Olwal, and Sean Follmer. Grability: A wearable haptic interface for simulating weight and grasping in virtual reality. In *Proceedings of the 30th Annual ACM Symposium on User Interface Software and Technology*, pages 119–130, 2017.
- [18] Inrak Choi, Elliot W Hawkes, David L Christensen, Christopher J Ploch, and Sean Follmer. Wolverine: A wearable haptic interface for grasping in virtual reality. In *2016 IEEE/RSJ International Conference on Intelligent Robots and Systems (IROS)*, pages 986–993. IEEE, 2016.
- [19] Alan B Craig. Understanding augmented reality. *Concepts and Applications*, 2013.
- [20] Heather Culbertson and Katherine J Kuchenbecker. Ungrounded haptic augmented reality system for displaying roughness and friction. *IEEE/ASME Transactions on Mechatronics*, 22(4):1839–1849, 2017.
- [21] Heather Culbertson, Cara M Nunez, Ali Israr, Frances Lau, Freddy Abnoui, and Allison M Okamura. A social haptic device to create continuous lateral motion using sequential normal indentation. In *2018 IEEE Haptics Symposium (HAPTICS)*, pages 32–39. IEEE, 2018.

- [22] Heather Culbertson, Samuel B Schorr, and Allison M Okamura. Haptics: The present and future of artificial touch sensation. *Annual Review of Control, Robotics, and Autonomous Systems*, 1:385–409, 2018.
- [23] Heather Culbertson, Julie M Walker, and Allison M Okamura. Modeling and design of asymmetric vibrations to induce ungrounded pulling sensation through asymmetric skin displacement. In *2016 IEEE Haptics Symposium (HAPTICS)*, pages 27–33. IEEE, 2016.
- [24] Heather Culbertson, Julie M Walker, Michael Raitor, and Allison M Okamura. Waves: a wearable asymmetric vibration excitation system for presenting three-dimensional translation and rotation cues. In *Proceedings of the 2017 CHI Conference on Human Factors in Computing Systems*, pages 4972–4982, 2017.
- [25] Sean Follmer, Daniel Leithinger, Alex Olwal, Akimitsu Hogge, and Hiroshi Ishii. inform: dynamic physical affordances and constraints through shape and object actuation. In *Uist*, volume 13, pages 2501988–2502032, 2013.
- [26] John W Garrett. The adult human hand: some anthropometric and biomechanical considerations. *Human factors*, 13(2):117–131, 1971.
- [27] Florian Gosselin, Tanguy Jouan, Julien Brisset, and Claude Andriot. Design of a wearable haptic interface for precise finger interactions in large virtual environments. In *First Joint Eurohaptics Conference and Symposium on Haptic Interfaces for Virtual Environment and Teleoperator Systems. World Haptics Conference*, pages 202–207. IEEE, 2005.
- [28] Ashley L Guinan, Nicholas C Hornbaker, Markus N Montandon, Andrew J Doxon, and William R Provancher. Back-to-back skin stretch feedback for communicating five degree-of-freedom direction cues. In *2013 World Haptics Conference (WHC)*, pages 13–18. IEEE, 2013.
- [29] Takuya Handa, Kenji Murase, Makiko Azuma, Toshihiro Shimizu, Satoru Kondo, and Hiroyuki Shinoda. A haptic three-dimensional shape display with three fingers grasping. In *2017 IEEE Virtual Reality (VR)*, pages 325–326. IEEE, 2017.
- [30] John Hardy, Christian Weichel, Faisal Taher, John Vidler, and Jason Alexander. Shapeclip: towards rapid prototyping with shape-changing displays for designers. In *Proceedings of the 33rd Annual ACM Conference on Human Factors in Computing Systems*, pages 19–28, 2015.
- [31] Seongkook Heo, Christina Chung, Geehyuk Lee, and Daniel Wigdor. Thor’s hammer: An ungrounded force feedback device utilizing propeller-induced propulsive force. In *Proceedings of the 2018 CHI Conference on Human Factors in Computing Systems*, pages 1–11, 2018.
- [32] Seki Inoue, Yasutoshi Makino, and Hiroyuki Shinoda. Active touch perception produced by airborne ultrasonic haptic hologram. In *2015 IEEE World Haptics Conference (WHC)*, pages 362–367. IEEE, 2015.

- [33] Ali Israr and Ivan Poupyrev. Tactile brush: drawing on skin with a tactile grid display. In *Proceedings of the SIGCHI Conference on Human Factors in Computing Systems*, pages 2019–2028, 2011.
- [34] Hiroo Iwata, Hiroaki Yano, Fumitaka Nakaizumi, and Ryo Kawamura. Project feelex: adding haptic surface to graphics. In *Proceedings of the 28th annual conference on Computer graphics and interactive techniques*, pages 469–476, 2001.
- [35] Saurabh Jadhav, Vikas Kannanda, Bocheng Kang, Michael T Tolley, and Jurgen P Schulze. Soft robotic glove for kinesthetic haptic feedback in virtual reality environments. *Electronic Imaging*, 2017(3):19–24, 2017.
- [36] Sungjune Jang, Lawrence H Kim, Kesler Tanner, Hiroshi Ishii, and Sean Follmer. Haptic edge display for mobile tactile interaction. In *Proceedings of the 2016 CHI Conference on Human Factors in Computing Systems*, pages 3706–3716, 2016.
- [37] Moon-Sub Jin and Jong-Il Park. Interactive mobile augmented reality system using a vibrotactile pad. In *2011 IEEE International Symposium on VR Innovation*, pages 329–330. IEEE, 2011.
- [38] Jingun Jung, Eunhye Youn, and Geehyuk Lee. Pinpad: touchpad interaction with fast and high-resolution tactile output. In *Proceedings of the 2017 CHI Conference on Human Factors in Computing Systems*, pages 2416–2425, 2017.
- [39] Chris D Kounavis, Anna E Kasimati, and Efpraxia D Zamani. Enhancing the tourism experience through mobile augmented reality: Challenges and prospects. *International Journal of Engineering Business Management*, 4:10, 2012.
- [40] Eun Kwon, Gerard J Kim, and Sangyoon Lee. Effects of sizes and shapes of props in tangible augmented reality. In *2009 8th IEEE International Symposium on Mixed and Augmented Reality*, pages 201–202. IEEE, 2009.
- [41] Daniel Leithinger, David Lakatos, Anthony DeVincenzi, Matthew Blackshaw, and Hiroshi Ishii. Direct and gestural interaction with relief: a 2.5 d shape display. In *Proceedings of the 24th annual ACM symposium on User interface software and technology*, pages 541–548, 2011.
- [42] Daniele Leonardis, Massimiliano Solazzi, Ilaria Bortone, and Antonio Frisoli. A wearable fingertip haptic device with 3 dof asymmetric 3-rsr kinematics. In *2015 IEEE World Haptics Conference (WHC)*, pages 388–393. IEEE, 2015.
- [43] Benjamin Long, Sue Ann Seah, Tom Carter, and Sriram Subramanian. Rendering volumetric haptic shapes in mid-air using ultrasound. *ACM Transactions on Graphics (TOG)*, 33(6):1–10, 2014.
- [44] Cristian Luciano, Pat Banerjee, Lucian Florea, and Greg Dawe. Design of the immersive-touch: a high-performance haptic augmented virtual reality system. In *11th international conference on human-computer interaction, Las Vegas, NV*, 2005.

- [45] Maurizio Maisto, Claudio Pacchierotti, Francesco Chinello, Gionata Salvietti, Alessandro De Luca, and Domenico Prattichizzo. Evaluation of wearable haptic systems for the fingers in augmented reality applications. *IEEE transactions on haptics*, 10(4):511–522, 2017.
- [46] Thomas H Massie and J Kenneth Salisbury. The phantom haptic interface: A device for probing virtual objects. In *Proceedings of the ASME winter annual meeting, symposium on haptic interfaces for virtual environment and teleoperator systems*, volume 55, pages 295–300. Chicago, IL, 1994.
- [47] Mark R Mine, Frederick P Brooks Jr, and Carlo H Sequin. Moving objects in space: exploiting proprioception in virtual-environment interaction. In *Proceedings of the 24th annual conference on Computer graphics and interactive techniques*, pages 19–26, 1997.
- [48] Taha K Moriyama, Ayaka Nishi, Rei Sakuragi, Takuto Nakamura, and Hiroyuki Kajimoto. Development of a wearable haptic device that presents haptics sensation of the finger pad to the forearm. In *2018 IEEE Haptics Symposium (HAPTICS)*, pages 180–185. IEEE, 2018.
- [49] Takaki Murakami, Tanner Person, Charith Lasantha Fernando, and Kouta Minamizawa. Altered touch: miniature haptic display with force, thermal and tactile feedback for augmented haptics. In *ACM SIGGRAPH 2017 Posters*, pages 1–2. 2017.
- [50] Takuya Nojima, Dairoku Sekiguchi, Masahiko Inami, and Susumu Tachi. The smarttool: A system for augmented reality of haptics. In *Proceedings IEEE Virtual Reality 2002*, pages 67–72. IEEE, 2002.
- [51] Claudio Pacchierotti, Gionata Salvietti, Irfan Hussain, Leonardo Meli, and Domenico Prattichizzo. The hring: A wearable haptic device to avoid occlusions in hand tracking. In *2016 IEEE Haptics Symposium (HAPTICS)*, pages 134–139. IEEE, 2016.
- [52] Claudio Pacchierotti, Stephen Sinclair, Massimiliano Solazzi, Antonio Frisoli, Vincent Hayward, and Domenico Prattichizzo. Wearable haptic systems for the fingertip and the hand: taxonomy, review, and perspectives. *IEEE transactions on haptics*, 10(4):580–600, 2017.
- [53] Riccardo Palmarini, John Ahmet Erkoyuncu, Rajkumar Roy, and Hosein Torabmostaedi. A systematic review of augmented reality applications in maintenance. *Robotics and Computer-Integrated Manufacturing*, 49:215–228, 2018.
- [54] Jérôme Perret and Emmanuel Vander Poorten. Touching virtual reality: a review of haptic gloves. In *ACTUATOR 2018; 16th International Conference on New Actuators*, pages 1–5. VDE, 2018.
- [55] Wayne Piekarski and Bruce H Thomas. *The tinmith system: demonstrating new techniques for mobile augmented reality modelling*, volume 24. Australian Computer Society, Inc., 2002.

- [56] Domenico Prattichizzo, Claudio Pacchierotti, and Giulio Rosati. Cutaneous force feedback as a sensory subtraction technique in haptics. *IEEE Transactions on Haptics*, 5(4):289–300, 2012.
- [57] Joseph M Romano and Katherine J Kuchenbecker. The airwand: design and characterization of a large-workspace haptic device. In *2009 IEEE International Conference on Robotics and Automation*, pages 1461–1466. IEEE, 2009.
- [58] Samuel Benjamin Schorr and Allison M Okamura. Three-dimensional skin deformation as force substitution: Wearable device design and performance during haptic exploration of virtual environments. *IEEE transactions on haptics*, 10(3):418–430, 2017.
- [59] Alexa F Siu, Eric J Gonzalez, Shenli Yuan, Jason B Ginsberg, and Sean Follmer. Shapeshift: 2d spatial manipulation and self-actuation of tabletop shape displays for tangible and haptic interaction. In *Proceedings of the 2018 CHI Conference on Human Factors in Computing Systems*, pages 1–13, 2018.
- [60] Rajinder Sodhi, Ivan Poupyrev, Matthew Glisson, and Ali Israr. Aireal: interactive tactile experiences in free air. *ACM Transactions on Graphics (TOG)*, 32(4):1–10, 2013.
- [61] Andrew A Stanley, James C Gwilliam, and Allison M Okamura. Haptic jamming: A deformable geometry, variable stiffness tactile display using pneumatics and particle jamming. In *2013 World Haptics Conference (WHC)*, pages 25–30. IEEE, 2013.
- [62] Shan-Yuan Teng, Tzu-Sheng Kuo, Chi Wang, Chi-huan Chiang, Da-Yuan Huang, Liwei Chan, and Bing-Yu Chen. Pupop: Pop-up prop on palm for virtual reality. In *Proceedings of the 31st Annual ACM Symposium on User Interface Software and Technology*, pages 5–17, 2018.
- [63] D. Tsetserukou, S. Hosokawa, and K. Terashima. Linktouch: A wearable haptic device with five-bar linkage mechanism for presentation of two-dof force feedback at the fingerpad. In *2014 IEEE Haptics Symposium (HAPTICS)*, pages 307–312, 2014.
- [64] James Vallino and Christopher Brown. Haptics in augmented reality. In *Proceedings IEEE International Conference on Multimedia Computing and Systems*, volume 1, pages 195–200. IEEE, 1999.
- [65] DWF Van Krevelen and Ronald Poelman. A survey of augmented reality technologies, applications and limitations. *International journal of virtual reality*, 9(2):1–20, 2010.
- [66] Petr Vávra, J Roman, Pavel Zonča, Peter Ihnát, Martin Němec, J Kumar, Nagy Habib, and A El-Gendi. Recent development of augmented reality in surgery: a review. *Journal of healthcare engineering*, 2017, 2017.
- [67] Ramiro Velazquez, Edwige Pissaloux, Moustapha Hafez, and Jérôme Szewczyk. A low-cost highly-portable tactile display based on shape memory alloy micro-actuators. In *IEEE Symposium on Virtual Environments, Human-Computer Interfaces and Measurement Systems, 2005.*, pages 6–pp. IEEE, 2005.

- [68] Robert J Webster III, Todd E Murphy, Lawton N Verner, and Allison M Okamura. A novel two-dimensional tactile slip display: design, kinematics and perceptual experiments. *ACM Transactions on Applied Perception (TAP)*, 2(2):150–165, 2005.
- [69] Rui Zhang, Andreas Kunz, Patrick Lochmatter, and Gabor Kovacs. Dielectric elastomer spring roll actuators for a portable force feedback device. In *2006 14th Symposium on Haptic Interfaces for Virtual Environment and Teleoperator Systems*, pages 347–353. IEEE, 2005.